Reflected in-plane conductance near a barrier with Dresselhaus spin-orbit coupling

Mou Yang
State Key Laboratory for Superlattices and Microstructures, Institute of Semiconductors, Chinese Academy of Sciences, P.O. Box 912, Beijing 100083, China

Shu-Shen Li*
CCAST (World Laboratory), P.O. Box 8730, Beijing 100080, and State Key Laboratory for Superlattices and Microstructures, Institute of Semiconductors, Chinese Academy of Sciences, P.O. Box 912, Beijing 100083, China

(Received 18 April 2005; revised manuscript received 18 July 2005; published 28 November 2005)

We have calculated the in-plane conductance of a barrier with the Dresselhaus spin-orbit interaction, which is sandwiched between two spin-polarized materials aligned arbitrarily. Besides a transmitted in-plane current which arises on the drain side as pointed out in Phys. Rev. Lett. **93**, 056601 (2004), a reflected in-plane current always appears simultaneously on the source side near the interface of the barrier. The spin polarization of the source affects the transmitted current more than the reflected one, and conversely the spin polarization of the drain affects the reflected current more. The relationship between transmitted current and the reflected one has been studied.

DOI: 10.1103/PhysRevB.72.193310 PACS number(s): 72.25.Dc, 72.25.Mk, 73.40.Gk

Electric transport properties of microstructures with Dresselhaus spin-orbit coupling[1] (SOC) and Rashba SOC (Ref. 2) have drawn much attention since Datta and Das proposed the spin-field effect transistor,[3] because SOC may provide a convenient way to manipulate the spin without introducing a magnetic field,[4] which is important for spin-based hardware techniques and future quantum computations. The SOC couples the spin of electrons with their motion, causes an additional channel for the decoherence and relaxation of electron spin,[5] induces spin procession in variety of physical systems,[6–8] and can be utilized to produce spin-polarized current.[4] In the two-dimensional electron (hole) system, the SOC can bring about a Hall-like spin current,[9–11] which has already been observed experimentally.[12,13] Recently, Tarasenko *et al.* proposed a scheme to produce a Hall-like *electric* current by means of the SOC in a thin barrier sandwiched between a spin-polarized material and a non-spin-polarized one.[14] They argued that an in-plane current parallel to the barrier interfaces on the drain side arises because the transmission of electrons depends on the orientation the of the in-plane component of their velocity. However, the authors have not noticed that the dependence of the transmission on it must lead to the conclusion that the reflection depends on it also. This dependence of the reflection results in another interface current appearing on the source side. Because either the transmitted interface (TI) current or the reflected interface (RI) current, or the sum of them, could be useful for the measurement of the SOC strength and the detection of spin-polarized carriers, the RI current is needed to be studied and compared with the TI current, and the relation between the two interface currents is needed to be clarified.

Motivated by the above, we consider a system in which two spin-polarized materials sandwich a thin layer barrier growing along the cubic crystallographic axis [001], where the Dresselhaus SOC works, similar to that in Ref. 14. When a dc bias is applied across the barrier, the TI and RI currents appear, respectively, on drain and source sides. A detailed discussion on the origination of the TI current can be found in Ref. 14 but it is not addressed here, whereas we demonstrate it visually in Fig. 1(a). As a glimpse suggests, it seems that the RI current should be against the TI current, because a larger transmission means a smaller reflection. But our calculation reveals that it is not true. In fact, the directions of the two interface currents form a common angle [see Fig. 1(b)]. The relation between the two currents is investigated, and some general results are obtained.

The barrier we consider here has a height V, a width a, and the Dresselhaus constant γ. If the barrier height is much higher than the Fermi level E_F, the Dresselhaus Hamiltonian in the barrier region reads[15]

$$H_D = \gamma(\sigma_x k_x - \sigma_y k_y)\frac{\partial^2}{\partial z^2}, \tag{1}$$

where σ is the Pauli matrix and $\mathbf{k}=(k_x,k_y,k_z)$ is the wave vector. The x, y, and z coordinate axes are set to be para-

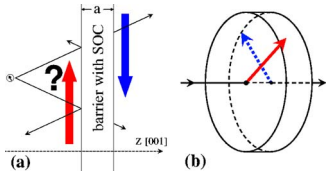

FIG. 1. (Color online) (a) A sketch for the origination of the in-plane currents nearby the barrier. The solid arrows denote the injection, transmission, and reflection of the electron. The relative magnitudes of transmission (reflection) for the upper path and the lower path are revealed by the length of these arrows. The blue and red arrows represent the TI and RI currents. The question mark means that the direction of the RI current should be considered carefully given that the TI current runs downward. (b) A sketch to show a possible configuration of the TI current (blue arrow) and RI current (red arrow), where the two interface currents do not run in opposite directions. The black arrows represent the current normal to the interface.

llel to the crystallographic axes [100], [010], and [001], respectively. The eigenspinors in the barrier region are $\chi_{\pm}=(1/\sqrt{2})(1,\pm e^{-i\varphi})^T$, where φ is the in-plane azimuth angle of $\mathbf{k}$ [i.e., $\mathbf{k}=(k_{\parallel}\cos\varphi, k_{\parallel}\sin\varphi, k_z)$ and $k_{\parallel}=(k_x^2+k_y^2)^{1/2}$]. The polarization axes of the left and right sides are set to be $\mathbf{n}_{\alpha}=(\sin\theta_{\alpha}\cos\phi_{\alpha}, \sin\theta_{\alpha}\sin\phi_{\alpha}, \cos\theta_{\alpha})$, where $\alpha=L$, R, and θ_{α} and ϕ_{α} are, respectively, the colatitude and azimuth angles of $\mathbf{n}_{\alpha}$. The spin splitting on each side is assumed to be $2h_0$.

The transport properties are determined by the transmission or the reflection matrix of electron at the Fermi level.[16] The transmission and reflection matrices for our system can be obtained using the scattering matrix method,[16,17] analogous to that in Ref. 17, while the details are not shown here. Because the transversal currents, not the longitudinal current, are the objects studied by us, it is convenient to define the in-plane transmission matrix $\mathcal{T}=(k_{\parallel}/\mathbf{K})^{1/2}\mathbf{t}$ and the in-plane reflection matrix $\mathcal{R}=(k_{\parallel}/\mathbf{K})^{1/2}\mathbf{r}$, where $\mathbf{t}$ and $\mathbf{r}$ are the transmission matrix and reflection matrix, and $\mathbf{K}=\mathrm{Diag}[k_{z\uparrow}, k_{z\downarrow}]$ is a diagonal matrix with $k_{z\uparrow}(k_{z\downarrow})$ being the z component of wave vector of spin-up (spin-down) electron (spin-up here is referred to as the spin orientation parallel to the spin polarization axis $\mathbf{n}_{\alpha}$). Given that the energy of the injected electron is E, $k_{z\uparrow}$ and $k_{z\downarrow}$ are, respectively, determined by $E=(\hbar^2/2m)(k_{z\uparrow}^2+k_{\parallel}^2)-h_0$ and $E=(\hbar^2/2m)(k_{z\downarrow}^2+k_{\parallel}^2)+h_0$, where m is the effective mass of electron. Finally, the two interface conductances (denoted, respectively, by $\mathbf{G}_t$ and $\mathbf{G}_r$ hereafter), caused by the transmitted and reflected electrons, can be calculated at zero temperature, which just have the Landauer form.[16,18] The x components of them are

$$(G_t)_x=\frac{l_R}{(2\pi)^2}\frac{e^2}{\hbar}\int_{E_F}\mathrm{Tr}[\mathcal{T}\mathcal{T}^{+}]\cos\varphi k_{\parallel}dk_{\parallel}d\varphi, \tag{2}$$

$$(G_r)_x=\frac{l_L}{(2\pi)^2}\frac{e^2}{\hbar}\int_{E_F}\mathrm{Tr}[\mathcal{R}\mathcal{R}^{+}]\cos\varphi k_{\parallel}dk_{\parallel}d\varphi, \tag{3}$$

where l_L (l_R) is the electron mean free length on the left (right) side. The y components of them can be obtained by replacing $\cos\varphi$ with $\sin\varphi$ in the above equations. Either the TI or RI conductance only exists near the barrier interface because of the momentum relaxation.

In this paper we are only interested in the weak tunneling case. We first consider the case that the spin polarizations of the source and drain are both in the x-y plane (i.e., $\theta_L=\theta_R=\pi/2$) and are aligned parallelly or antiparallelly, because the simple case contains much information for our further consideration of some complicated cases. After a certain calculation, we obtain

$$\begin{aligned}\widetilde{\mathbf{G}}_t&=\mathbf{n}_L l_R G_P \quad \text{for parallel alignment},\\ \widetilde{\mathbf{G}}_t&=\mathbf{n}_L l_R G_{AP} \quad \text{for antiparallel alignment},\end{aligned} \tag{4}$$

where $\widetilde{\mathbf{A}}$ denotes the mirror image of vector $\mathbf{A}$ about the x axis—namely, $\widetilde{\mathbf{A}}_x=\mathbf{A}_x$ and $\widetilde{\mathbf{A}}_y=-\mathbf{A}_y$. In the following we will be concerned with $\widetilde{\mathbf{G}}_t$ instead of $\mathbf{G}_t$. G_P and G_{AP} are two integrals, which determine the amplitudes of the TI conductance for the parallel and antiparallel configurations, respectively:

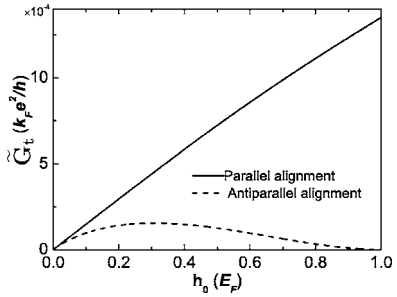

FIG. 2. Curves of $\widetilde{G}_t$ vs h_0 for parallel and antiparallel alignments. The parameters are $\theta_L=\theta_R=\pi/2$, $V=10E_F$, $a=\lambda_F/4$, $(2m/\hbar^2)k_F\gamma=0.01$, and $l_0=10^3\lambda_F$.

$$G_P=\frac{1}{2\pi}\frac{e^2}{h}\int_{E_F}\frac{1}{4}\Big[(|t_{\uparrow+\uparrow}|^2-|t_{\uparrow-\uparrow}|^2)\frac{k_{\parallel}}{k_{z\uparrow}} -(|t_{\downarrow+\downarrow}|^2-|t_{\downarrow-\downarrow}|^2)\frac{k_{\parallel}}{k_{z\downarrow}}\Big]k_{\parallel}dk_{\parallel}, \tag{5}$$

$$G_{AP}=\frac{1}{2\pi}\frac{e^2}{h}\int_{E_F}\frac{1}{4}\Big[(|t_{\downarrow+\uparrow}|^2-|t_{\downarrow-\uparrow}|^2)\frac{k_{\parallel}}{k_{z\uparrow}} -(|t_{\uparrow+\downarrow}|^2-|t_{\uparrow-\downarrow}|^2)\frac{k_{\parallel}}{k_{z\downarrow}}\Big]k_{\parallel}dk_{\parallel}, \tag{6}$$

where $t_{\nu\pm\mu}$ ($\mu=\uparrow,\downarrow$ and $\nu=\uparrow,\downarrow$) is the transmission coefficient of an electron injected from the left with the spin-μ state, propagating in the eigenchannel $\chi_{\pm}$ in the barrier, and finally going out to the right side with the spin-ν state. Figure 2 shows the curves of the magnitude of $\widetilde{\mathbf{G}}_t$ as functions of h_0 for the parallel and antiparallel configurations (λ_F and k_F in the figure are the Fermi wavelength and Fermi wave vector, respectively). It implies that the TI conductance for parallel alignment increases monotonically with increasing h_0 but that for antiparallel alignment has a maximum at certain h_0, and the former is larger than the latter. A similar conclusion can be drawn about the behaviors of G_P and G_{AP} when h_0 varies, because they are proportional to the amplitudes of TI conductances for parallel and antiparallel alignments.

If the polarization of the source and drain are aligned arbitrarily, the TI conductance can also be easily obtained by applying the weak tunneling approximation in Eq. (2). After some tedious calculations, we have

$$\widetilde{\mathbf{G}}_t=l_R(G_{+}\mathbf{n}_L^{\parallel}+G_{-}\mathbf{n}_R^{\parallel}), \tag{7}$$

where $G_{\pm}=(G_P\pm G_{AP})/2$ and $\mathbf{n}_{\alpha}^{\parallel}$ is the projection of $\mathbf{n}_{\alpha}$ on the x-y plane with $n_{\alpha}^{\parallel}=n_{\alpha}\sin\theta_{\alpha}$. Equation (7) implies that the TI conductance for an arbitrary configuration is the mixture of that for a parallel configuration and that for an antiparallel configuration, which can be seen more clearly if we rewrite Eq. (7) as $\widetilde{\mathbf{G}}_t=\frac{1}{2}l_R[G_P(\mathbf{n}_L^{\parallel}+\mathbf{n}_R^{\parallel})+G_{AP}(\mathbf{n}_L^{\parallel}-\mathbf{n}_R^{\parallel})]$. The RI conductance can be calculated straightforward by using Eq. (3). Before we carry out the calculation, we launch a discussion about the relation between the two interface con-

ductances to acquire some general properties of them. If there is no bias across the barrier, apparently no current flows across the barrier and no interface current flows nearby the barrier as well. We can understand this in two different ways. One viewpoint is that no electron can tunnel through the barrier because there is no room on the opposite side to accommodate it, so no current arises. The other is that the electrons can tunnel from each side to the other side, but all the physical observables accompanied with the opposite tunneling processes cancel each other. The two views are the same from the physical viewpoint. So the RI current contributed by the electrons injected from the left with an energy E must be canceled by the TI current caused by the electrons injected from the right with the same energy. The above argument is not only precisely correct in the free-electron frame, but also correct if the electron-electron interaction is taken into account. Therefore we need not calculate the RI conductance over again as we calculated the TI one. Instead, we calculate TI conductance with the opposite injection using the already obtained Eq. (7). Reversing the newly obtained TI conductance, we obtain the RI conductance as

$$\tilde{\mathbf{G}}_r = -\tilde{\mathbf{G}}_t^{rev} = -l_L(G_+\mathbf{n}_R^{\parallel} + G_-\mathbf{n}_L^{\parallel}), \tag{8}$$

where $\mathbf{G}_t^{rev}$ is the TI conductance with reversed voltage bias across the barrier.

Equations (7) and (8) imply that the TI and RI conductances are determined by both the spin polarization of the source and that of the drain. Because G_+ is always larger than G_-, the TI conductance is affected more by polarization of the source and the RI conductance is affected more by that of the drain. The two interface conductances reach their respective maximum values for the parallel alignment and reach their respective minimum values for the antiparallel configuration. The two interface conductances may orient oppositely, run in the same direction, or have a common angle, depending on the relative configurations of $\mathbf{n}_L$ and $\mathbf{n}_R$ (the mean free lengths on the two sides are assumed to be identical—namely, $l_L=l_R=l_0$, hereafter). Especially, if $\theta_R=0$, we have $\tilde{\mathbf{G}}_t=l_0G_+\mathbf{n}_L^{\parallel}$; thus, we reproduce the result in Ref. 14. In this case the image of the RI conductance is $\tilde{\mathbf{G}}_r=-l_0G_-\mathbf{n}_L^{\parallel}$, but it was totally overlooked in Ref. 14. Figure 3 shows the evolution of $\tilde{\mathbf{G}}_t$ and $\tilde{\mathbf{G}}_r$ when $\phi_L=\pi/4$ and ϕ_R varies within $0\sim2\pi$. One can see that the evolution loops of the TI conductance and the RI conductance are two circles. It can be understood from Eqs. (7) and (8) by means of the triangle rule for vector addition. Because ϕ_α is the azimuth angle of $\mathbf{n}_\alpha$, that ϕ_L is fixed means the vectors $l_0G_+\mathbf{n}_L^{\parallel}$ in Eq. (7) and $-l_0G_-\mathbf{n}_L^{\parallel}$ in Eq. (8) (represented, respectively, by arrows 2 and 3 in Fig. 3) are fixed and that ϕ_R varies from 0 to 2π means the vectors $l_0G_-\mathbf{n}_R^{\parallel}$ in Eq. (7) and $-l_0G_+\mathbf{n}_R^{\parallel}$ in Eq. (8) (represented, respectively, by arrows 1 and 4 in Fig. 3) rotate anticlockwise. According to the triangle rule, the evolution loops are two circles with centers determined by arrows 2 and 3 and radii determined by arrows 1 and 4. Though only the case of zero temperature is considered in this paper, the calculations can be extended to the nonzero-temperature case as soon as the dependence of the mean free length on the temperature is known.

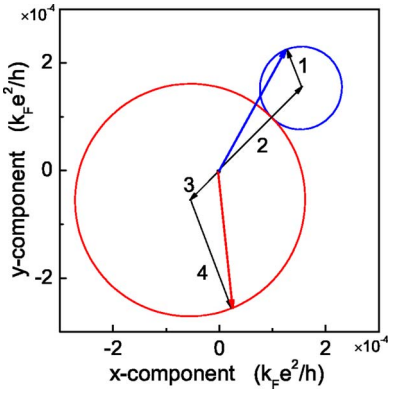

FIG. 3. (Color online) Evolution loops of $\tilde{\mathbf{G}}_t$ (blue curve) and $\tilde{\mathbf{G}}_r$ (red curve) when ϕ_L is fixed at $\pi/4$ and ϕ_R varies from 0 to 2π. The parameters are $\theta_L=\theta_R=\pi/2$, $V=10E_F$, $a=\lambda_F/4$, $(2m/\hbar^2)k_F\gamma=0.01$, $h_0=0.2E_F$, and $l_0=10^3\lambda_F$. The blue and red arrows represent, respectively, the vectors $\tilde{\mathbf{G}}_t$ and $\tilde{\mathbf{G}}_r$. The triangles show how $\tilde{\mathbf{G}}_t$ and $\tilde{\mathbf{G}}_r$ can be obtained from Eqs. (7) and (8) via the triangle rule for vector addition. The arrows labeled by 1, 2, 3, and 4 denote the vectors $l_0G_-\mathbf{n}_R^{\parallel}$, $l_0G_+\mathbf{n}_L^{\parallel}$, $-l_0G_-\mathbf{n}_L^{\parallel}$, and $-l_0G_+\mathbf{n}_R^{\parallel}$ appearing in Eqs. (7) and (8), respectively. The fixation of ϕ_L means the fixation of vectors 2 and 3, and the variation of ϕ_R means the rotation of vectors 1 and 4.

The Rashba SOC term, which reads[19]

$$(\hbar/2m_ec)^2(E_{SD}/a)(\sigma_xk_y-\sigma_yk_x),$$

can also cause interface currents,[14] where m_e, c, and E_{SD} are, respectively, the mass of the electron, velocity of light, and difference of the Fermi levels in the left and right sides, while the Dresselhaus term is the predominate one in the barrier region if the barrier height is much higher than the Fermi level and $E_{SD}<V$. One can check this argument by comparing the factor $(\hbar/2m_ec)^2E_{SD}/a$ in the Rashba term with the factor $\gamma\partial^2/\partial z^2$ in the Dresselhaus term with all parameters specified as typical values.[15] Thus, the interface currents induced by the Rashba term are much smaller and do not enter our calculations.

If the source and drain are Mn-doped InAs (Ref. 20) with spin polarization 50%–60%, (Ref. 21) Fermi energy 0.017 eV, and mean free length 10 μm and if the barrier is GaAs ($\gamma=2.4\times10^{-29}$ eV m^3) with barrier width 8 nm, the RI and TI conductances are of the order of 10^{-6} A/cm for parallel alignment and 10^{-7} A/cm for antiparallel alignment (assuming the spin polarization axes are in the x-y plane).[22]

Finally, we demonstrate why the orientation of the RI current is not opposite to that of the TI one from another perspective. The reflection of electrons injected along the upper path is assuredly smaller than that injected along the lower one if the transmission of the former case is larger than that of the latter, just as depicted in Fig. 1(a). But this is not enough to determine the orientation of the RI current. For example, given that the injected electron is spin up, the reflection probability has two components $|\mathbf{r}_{\uparrow\uparrow}|^2$ and $|\mathbf{r}_{\downarrow\uparrow}|^2$, the probabilities of the electron reflected into the spin-up

channel and spin-down channel, respectively. The reflection probability is the sum of the two components—namely, $|\mathbf{r}_{\uparrow\uparrow}|^2+|\mathbf{r}_{\downarrow\uparrow}|^2$. The RI current contributed by the injected electron is not proportional to the reflection probability, but is proportional to the in-plane reflection probability $|\mathcal{R}_{\uparrow\uparrow}|^2+|\mathcal{R}_{\downarrow\uparrow}|^2=(k_{\|}/k_{z\uparrow})|\mathbf{r}_{\uparrow\uparrow}|^2+(k_{\|}/k_{z\downarrow})|\mathbf{r}_{\downarrow\uparrow}|^2$. One can see that $(|\mathbf{r}_{\uparrow\uparrow}|^2+|\mathbf{r}_{\downarrow\uparrow}|^2)_{upper}<(|\mathbf{r}_{\uparrow\uparrow}|^2+|\mathbf{r}_{\downarrow\uparrow}|^2)_{lower}$ cannot guarantee $(|\mathcal{R}_{\uparrow\uparrow}|^2+|\mathcal{R}_{\downarrow\uparrow}|^2)_{upper}<(|\mathcal{R}_{\uparrow\uparrow}|^2+|\mathcal{R}_{\downarrow\uparrow}|^2)_{lower}$. So the result is somewhat contradictory to the conclusion drawn at the first sight.

In summary, we have investigated the in-plane transport properties of the system consisting of two spin-polarized materials sandwiching a barrier with the Dresselhaus SOC. The RI conductance, which was not noticed in Ref. 14 and the TI conductance are mainly affected by the spin polarization of the drain and that of the source, respectively. Contrary to one's intuition, the orientations of two interface conductances are not opposite, but form a common angle. The relationship between the two conductances has also been discussed.

This work was supported by the National Natural Science Foundation of China and the special Foundation for State Major Basic Research Program of China under Grant No. G2001CB309500.

*Corresponding author. Electronic address: sslee@red.semi.ac.cn

[1] G. Dresselhaus, Phys. Rev. **100**, 580 (1955).
[2] E. I. Rashba, Fiz. Tverd. Tela (Leningrad) **2**, 1224 (1960).
[3] S. Datta and B. Das, Appl. Phys. Lett. **56**, 665 (1990).
[4] A. Voskoboynikov, S. S. Liu, and C. P. Lee, Phys. Rev. B **58**, 15397 (1998).
[5] I. Žutić, J. Fabian, and S. D. Sarma, Rev. Mod. Phys. **76**, 323 (2004).
[6] J. Wang, H. B. Sun, and D. Y. Xing, Phys. Rev. B **69**, 085304 (2004).
[7] R. Winkler, Phys. Rev. B **69**, 045317 (2004).
[8] M. Valín-Rodríguez, A. Puente, L. Serra, and E. Lipparini, Phys. Rev. B **66**, 235322 (2002).
[9] S. Murakami, N. Nagaosa, and S. C. Zhang, Science **301**, 1348 (2003).
[10] J. Sinova, D. Culcer, Q. Niu, N. A. Sinitsyn, T. Jungwirth, and A. H. MacDonald, Phys. Rev. Lett. **92**, 126603 (2004).
[11] S. Q. Shen, M. Ma, X. C. Xie, and F. C. Zhang, Phys. Rev. Lett. **92**, 256603 (2004).
[12] Y. K. Kato, R. C. Myers, A. C. Gossard, and D. D. Awschalom, Science **306**, 1910 (2004).
[13] J. Wunderlich, B. Käestner, J. Sinova, and T. Jungwirth, Phys. Rev. Lett. **94**, 047204 (2005).
[14] S. A. Tarasenko, V. I. Perel', and I. N. Yassievich, Phys. Rev. Lett. **93**, 056601 (2004).
[15] V. I. Perel', S. A. Tarasenko, I. N. Yassievich, S. D. Ganichev, V. V. Bel'kov, and W. Prettl, Phys. Rev. B **67**, 201304(R) (2003).
[16] S. Datta, *Electronic Transport in Mesoscopic Systems* (Cambridge University Press, Cambridge, England, 1997).
[17] F. Kassubek, C. A. Stafford, and H. Grabert, Phys. Rev. B **59**, 7560 (1999).
[18] Y. Imry and R. Landauer, Rev. Mod. Phys. **71**, 306 (1999).
[19] Q. F. Sun, J. Wang, and H. Guo, Phys. Rev. B **71**, 165310 (2005).
[20] D. Chiba, M. Yamanouchi, F. Matsukura, and H. Ohno, Science **301**, 943 (2003).
[21] The spin polarization of Mn-doped semiconductors varies within 0–100%, depending on the concentration of Mn [J. G. Braden, J. S. Parker, P. Xiong, S. H. Chun, and N. Samarth, Phys. Rev. Lett. **91**, 056602 (2003)].
[22] Because the barrier height is much greater than the Fermi energy, the influence of the Dresselhaus SOC on the motion of the electrons in the barrier region is much greater than in the source and the drain. Therefore, only the SOC in the barrier was considered for the example, though the Dresselhaus constants of InAs and GaAs are of the same order (Ref. 15).